Journal of Inorganic and Organometallic Polymers and Materials
https://doi.org/10.1007/s10904-024-03033-3

RESEARCH

Entropy Barrier Mitigation and Harnessing Localized Upcycled Graphene Nanoplatelets in Polypropylene/High-Density Polyethylene Nanoblends

Gülayşe Şahin Dündar[1,2] · **Burcu Saner Okan**[1,2]

Received: 19 December 2023 / Accepted: 5 February 2024
© The Author(s) 2024

Abstract
In pursuit of a sustainable future, the focus on thermoplastic compounding emerges as a transformative avenue. Strategically blending and compounding thermoplastics unlock the potential for eco-friendly materials, addressing pressing environmental concerns. Polymer blending is a widely utilized technique that offers significant advantages in terms of cost-effectiveness and the development of materials with diverse properties. However, achieving compatibility between polymers remains a challenge due to their non-negligible entropy, particularly in the case of immiscible polymers like Polypropylene (PP) and High-Density Polyethylene (HDPE). The success of such systems heavily depends on optimizing factors such as additive selection, mixing methodology, composition, and processing conditions. Despite the extensive industrial usage of polymers like PP and HDPE, there is still limited understanding regarding the impact of blending these polymers, especially when graphene is introduced. This study addresses these challenges by overcoming the entropy barrier between PP and HDPE using a high shear rate thermo-kinetic mixer and employing upcycled graphene nanoplatelets (GNP) as a type of low-cost graphene material through interface engineering. The GNP content in the blends ranged from 0 to 1 wt%, and through meticulous selection of the polymer weight fraction and the use of minimal GNP content, GNP was strategically localized at the blend interface. This resulted in remarkable mechanical performance achieved through the optimized manufacturing technique. Incorporating 0.1 wt% GNP resulted in a significant 38% increase in tensile modulus, while flexural modulus and flexural strength saw respective increments of 39% and 22% compared to neat PP. Further enhancements were observed with higher GNP contents. This study illuminates the transformative potential of thermoplastic compounding as a key driver toward a sustainable future.

✉ Burcu Saner Okan
burcu.saner@sabanciuniv.edu

[1] Faculty of Engineering and Natural Sciences, Materials Science and Nano Engineering, Sabanci University, 34956 Orhanli-Tuzla, Istanbul, Turkey

[2] Sabanci University Integrated Manufacturing Technologies Research and Application Center & Composite Technologies Center of Excellence, Teknopark Istanbul, 34906 Pendik, Istanbul, Turkey

Published online: 17 March 2024

Graphical Abstract

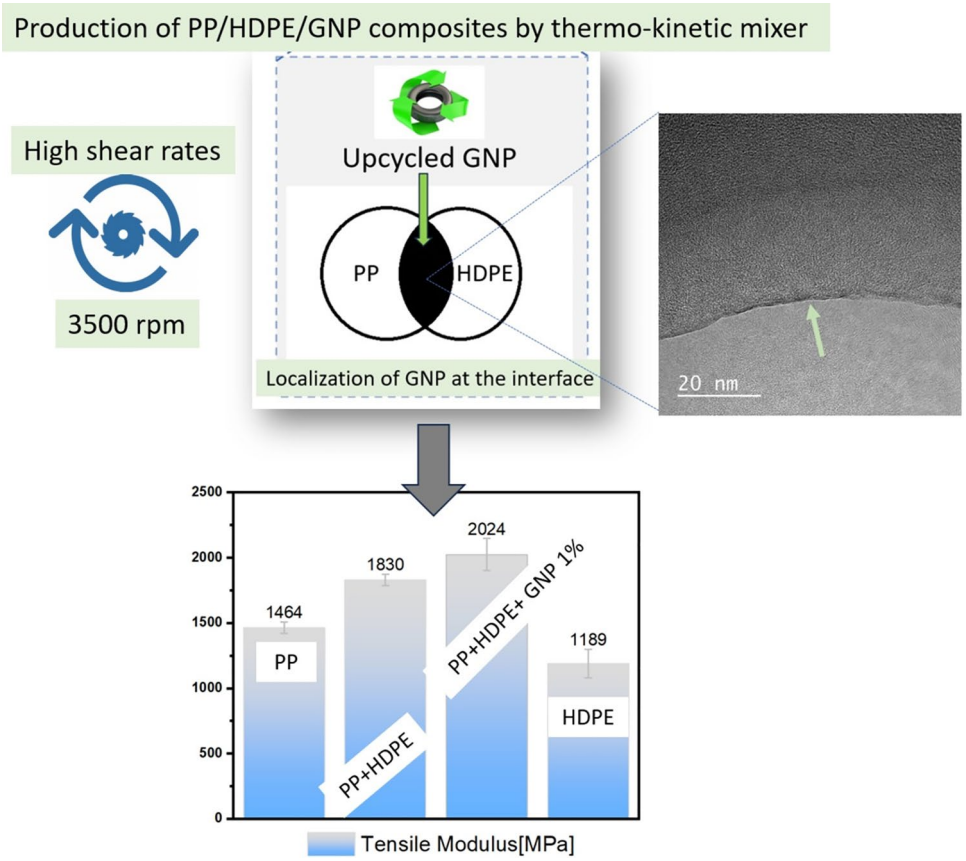

Keywords Polypropylene · High-density polyethylene · Graphene nanoplatelets · Nanocomposite · Polymer blends

1 Introduction

Thermoplastic compounding heralds a path toward enhanced sustainability, where innovative formulations pave the way for a greener and more resilient future. The production of polymer blends is a commonly employed technique to enhance the performance of polymers and is considered to be economically advantageous [1]. The economic benefits of polymer blends arise from the ability to leverage the favorable properties of two existing materials through mixing, rather than resorting to the synthesis of new materials. However, in practice, the problem of the incompatibility of polymer blends is often encountered [2]. Most polymers are immiscible and they do not mix homogeneously with each other due to their inherent and unfavorably low mixing entropy [3]. Polypropylene (PP) and Polyethylene (PE) are among these immiscible polymers as commodity plastics, and there have been few attempts to improve the compatibility of PE and PP, typically by adding a third component [4]. Graziano et al. used 2 wt% of reduced graphene oxide (RGO) in PE/PP blend resulting in finer droplet-matrix morphology [5]. In another study, they dispersed functional graphene at the interface of the PE/PP blend and improved the thermo-mechanical properties of the nanocomposites [6]. There are studies showing that polymer droplet diameters get smaller, especially if the localization of nanoparticles at the interface of two polymers can be achieved [7–9]. Studies demonstrate that nanoparticles can enhance the compatibility of polymer blends by reducing the surface tension [10]. Recently, graphene and derivatives have been used to improve the compatibility of different polymer blend systems [11–13]. Bera et al. used RGO for compatibilization of poly (vinylidene fluoride) (PVDF) and thermoplastic polyurethane (TPU) blend resulting in finer distributed holes [14]. The effectiveness of RGO in reducing the interfacial tension between the two polymers and promoting compatibilization suggests its potential as a viable substitute for traditional compatibilizers when blending otherwise incompatible polymers. In another study, thermally reduced graphene oxide (TRG) was selectively localized at the interface of the PP and PE blend by tailoring processing

sequences [15]. The lower interfacial tension of TRG with PE prompts its localization in PE within the PP/PE blend; however, when subjected to pre-blending with PP followed by the addition of PE, it can be localized at the interface.

Another parameter that affects the compatibility of polymer blends is the kinetic and process-related parameters, as temperature, shear force, screw design, and, speed also play a significant role in achieving a homogeneous distribution [16]. Therefore, blend morphology can be tailored by choosing the right manufacturing techniques and equipment. In a study, GNP localization at the interface of a polymer blend was controlled by melt-compounding sequences, mixing times, and, shear rates [8]. The conventional production method for melt blending of polymers is twin-screw extrusion [17]. It involves the melting of polymers along with additives by exceeding their melting temperature using twin rotating screws with co-rotating or counter-rotating designs tailored to desired characteristics. On the other hand, another production method, known as thermo-kinetic mixer, can offer advantages such as improved dispersion of fillers at high shear rates (3500–4500 rpm) and shorter production cycles (30 s), leading to better dispersion and distribution compared to conventional extrusion [18] and other type of internal mixers [19]. The thermo-kinetic mixer, especially, facilitates the easier exfoliation of nanofillers between polymer chains and prevents agglomeration issues encountered during polymer processing [20]. Therefore, morphology investigation on polymer blends by using a thermo-kinetic mixer can be effective in exploring blend compatibility, as the majority of previous polymer blend studies have primarily focused on twin-screw extrusion processes when melt compounding is under focus [16, 21– 25].

Herein, PP/HDPE binary blends and PP/HDPE/GNP ternary nanoblends were produced using a high shear rate thermo-kinetic mixer, and their mechanical, rheological, and morphological analysis were conducted to investigate compatibilization of the blend system. Results showed that by choosing the right manufacturing technique and the optimum GNP loading, GNP can be localized at the interface of the binary blends and improve the blend performance in terms of mechanical properties. The incorporation of upcycled graphene nanoplatelets (GNP) derived from waste tires is a deliberate choice with profound implications for environmental sustainability. Utilizing waste tires as a source of graphene not only addresses the global challenge of tire disposal but also transforms a potential environmental hazard into a valuable resource. Additionally, the PP/HDPE blend matrix can be an alternative matrix to solely homo PP since the synergistic effect of this blend showed higher mechanical properties compared to neat PP and HDPE. Along with this, the addition of GNP at 0.1 wt% resulted in a 38% increase in tensile modulus, while 39 and 22% increases in flexural modulus and flexural strength were achieved, respectively. Further enhancement was achieved by increasing GNP content to 1 wt%. Therefore, this study provided a low-cost blend formulation for industrial applications by changing the matrix composition from a more expensive homo PP to a cheaper blend of PP/HDPE by improving the mechanical behavior via an adaptable processing technique. The utilization of upcycled graphene nanoplatelets (GNP) from waste tires contributes to a circular economy by repurposing discarded materials. The integration of waste tire-derived GNP in thermoplastic blends not only minimizes environmental impact but also promotes resource efficiency. By highlighting the synergy between waste tire-driven GNP and thermoplastics, our study emphasizes a novel avenue for achieving advanced material properties while simultaneously addressing the importance of improving the compatibility and processing of PP and HDPE blends.

2 Materials and Methods

2.1 Materials

Homo Polypropylene (PP) with a density of 905 kg/m^3 and melt flow rate of (MFR) 12 g/10 min (230 °C/2.16 kg) was supplied by Borealis, Austria. High-density Polyethylene with a density of 965 kg/m^3 and melt flow rate of (MFR) 5.5 g/10 min (190 °C/2.16 kg) was supplied by PETKIM. Unmodified waste tire-derived graphene nanoplatelet (GNP) containing carbon (at.%: 87), oxygen (at.%: 9), and other elements (at.%: 4) was supplied by NANOGRAFEN Co., Kocaeli, Turkey.

2.2 Manufacturing of Polymer Blends

Manufacturing of all binary blends and ternary nanoblends was carried out in a melt phase, at 3500–4000 rpm and 200 °C by using a custom-made Gelimat-Thermo-kinetic Mixer (Dusatec Co, USA).

2.3 Characterization

2.3.1 Mechanical Properties

Specimens for tensile and flexural tests were prepared by lab-scale injection molding at 180° according to the ISO 527-2 and ISO 178 standards. The mechanical tests were conducted using Instron 5982 Static Universal Test Machine (UTM) for tensile and three-point bending tests according to the ISO 527-2 and ISO 178 standards. The average value of four test results was reported.

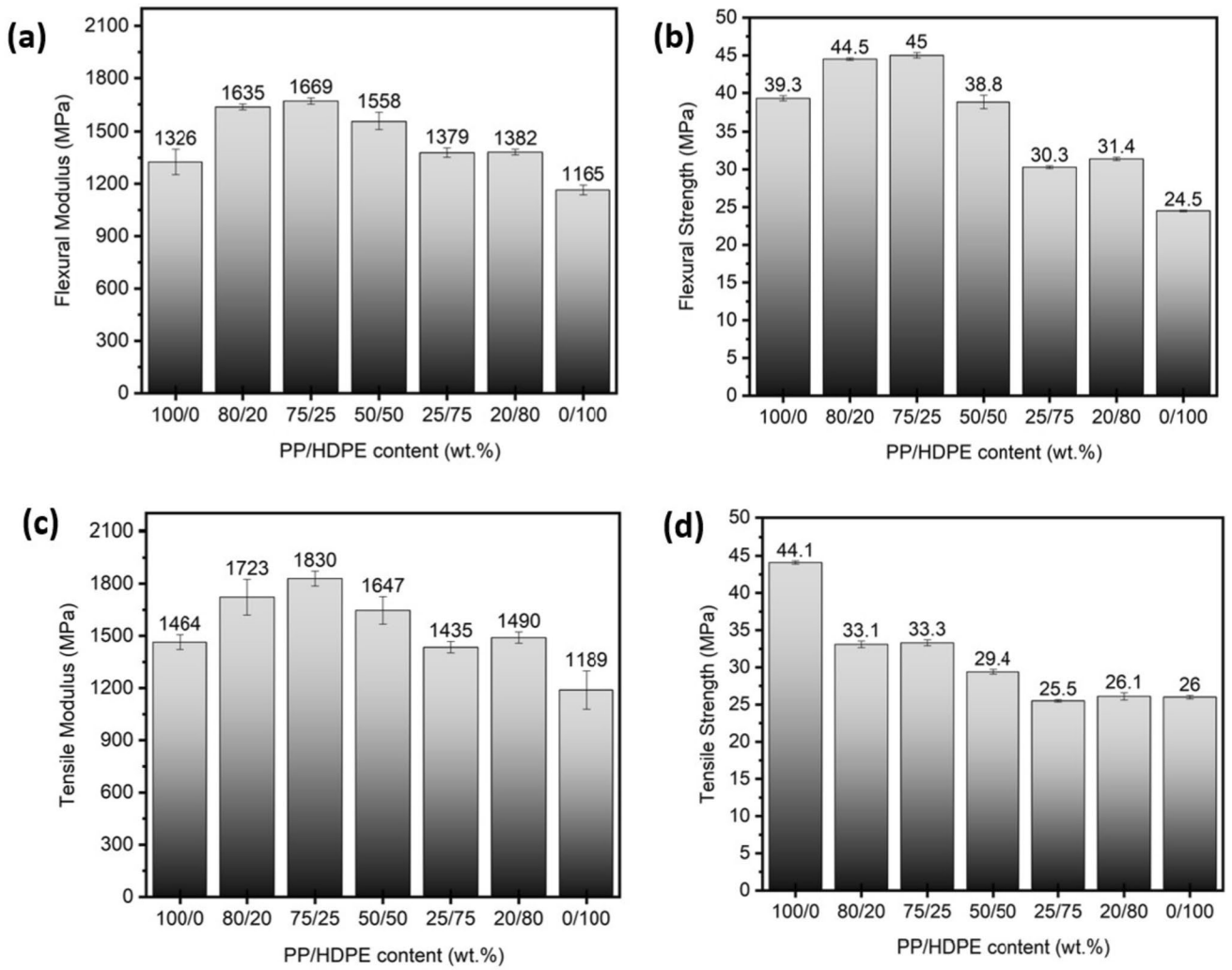

Fig. 1 **a** Flexural modulus, **b** flexural strength, **c** tensile modulus, and **d** tensile strength of binary polymer blends

2.3.2 Viscoelasticity and Dynamic Mechanical Properties

Dynamic Mechanical Analyzer (DMA) (Mettler Toledo, Columbus, OH, USA) was used to investigate the viscoelasticity of composites via a single cantilever bending from − 20 to 100 °C with 1 Hz frequency and 3 K/min heating rate.

2.3.3 Thermal Properties

Thermal analysis was investigated by Differential Scanning Calorimetry (DSC) 3 + 700 (Mettler Toledo, Columbus, OH, USA) under nitrogen gas with a 10 °C/ min heating rate.

2.3.4 Rheological Measurements

Frequency sweep tests were performed in Anton-Paar MCR 702 Rheometer using a parallel plate at 230 °C and strain of 1% in an angular frequency range of 1–1000 rad/s.

2.3.5 Morphological Analysis

Nikon Eclipse LV100ND was used for semi-polarized optical images. Freeze-fractured surfaces were examined under a Leo Supra 35VP Field Emission Scanning Electron Microscope (FESEM) by coating cross-sections with a thin layer of gold. Optical microscope images were taken by using the CLEMEX Image Analyzer System. Transmission Electron Microscopy (TEM) was conducted to examine the distribution of GNP in ternary nanoblends at varying loading levels, ranging from the lowest to the highest.

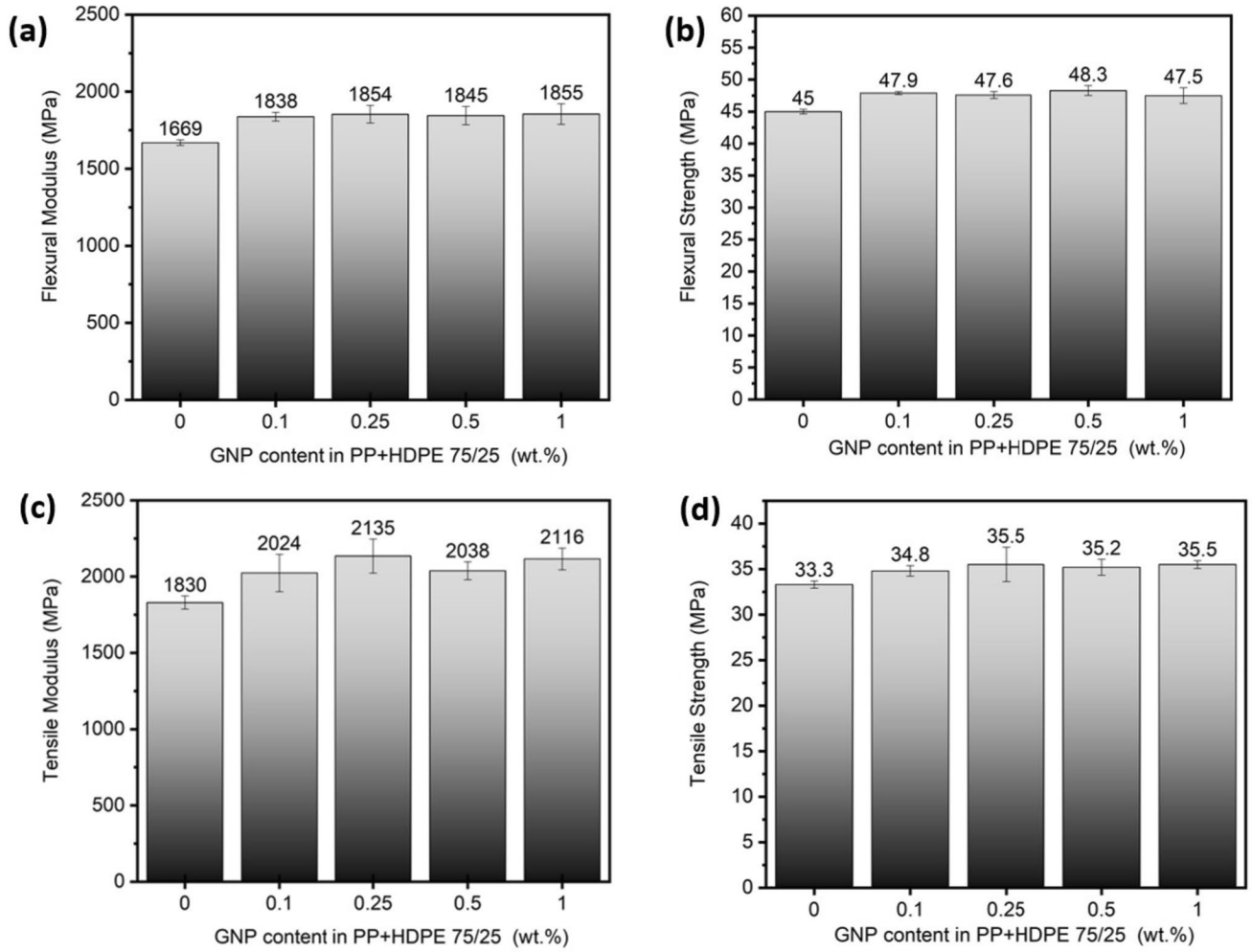

Fig. 2 **a** Flexural modulus, **b** flexural strength, **c** tensile modulus, and **d** tensile strength of ternary nanoblends

Table 1 Overall mechanical comparison and improvement of ternary nanoblends compared to PP + HDPE 75/25 and neat PP

Sample name	Compared to PP + HDPE 75/25	Compared to Neat PP	Compared to PP + HDPE 75/25	Compared to Neat PP
	Tensile modulus improvement (%)		Tensile strength improvement (%)	
PP + HDPE 75/25 GNP-0.1	11	38	5	–
PP + HDPE 75/25 GNP-0.25	17	46	7	–
PP + HDPE 75/25 GNP-0.5	11	39	6	–
PP + HDPE 75/25 GNP-1	16	45	7	–
	Flexural modulus improvement (%)		Flexural strength improvement (%)	
PP + HDPE 75/25 GNP-0.1	10	39	6	22
PP + HDPE 75/25 GNP-0.25	11	40	6	21
PP + HDPE 75/25 GNP-0.5	11	39	7	23
PP + HDPE 75/25 GNP-1	11	40	6	21

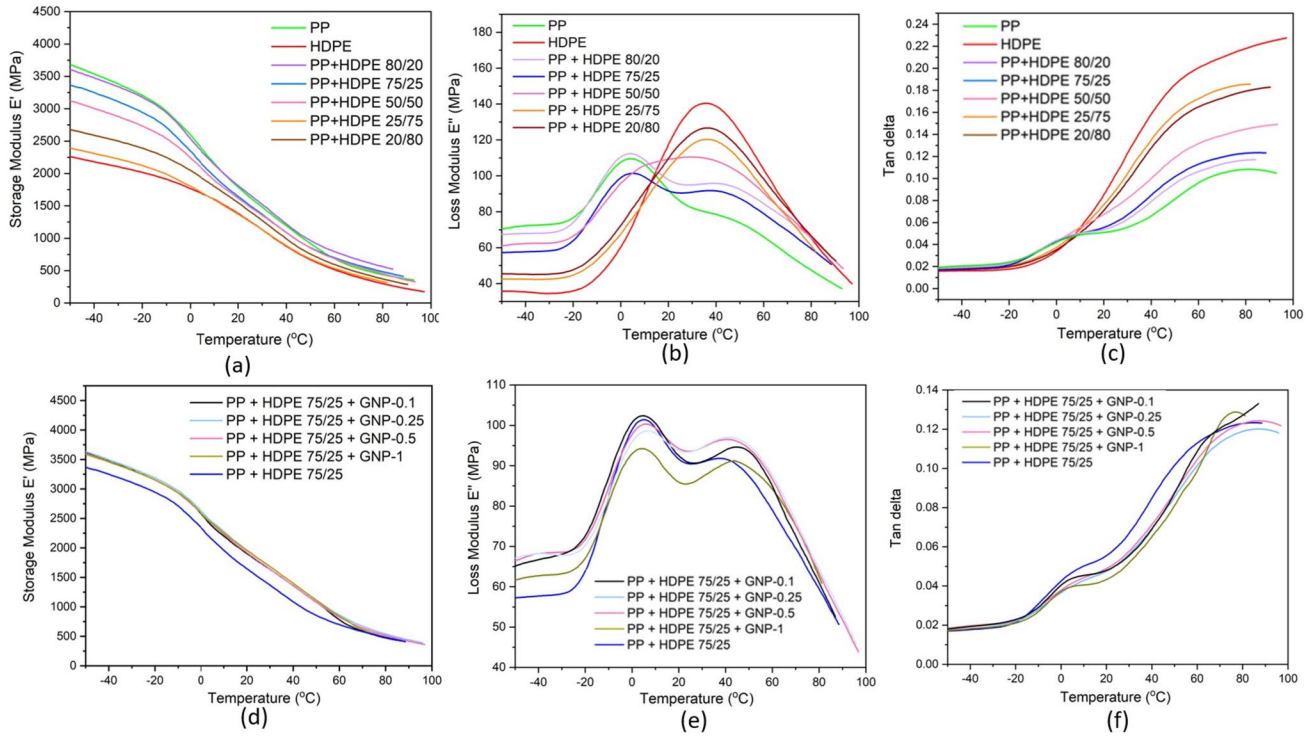

Fig. 3 **a**, **d** storage modulus; **b**, **e** loss modulus; **c**, **f** tan delta of binary blends and ternary nanoblends by DMA

3 Results and Discussion

3.1 Mechanical Behaviour of Binary Blends and Ternary Nanoblends

Polymer blends were produced by adding HDPE to PP at varying loading ratios (20–80 wt%) via a thermo-kinetic mixer. The mechanical results of the PP/HDPE polymer blends are shown in Fig. 1. When examining the flexural modulus values, all blend formulations showed higher results compared to neat PP. In particular, the PP + HDPE 75/25 blend exhibited the highest result at 1669 MPa, representing a 26% increase compared to neat PP. Similarly, the same formulation showed the highest flexural strength with 45 MPa. The tensile modulus also exhibited the highest value of 1830 MPa, indicating a 25% increase compared to neat PP. The tensile strength value was 33.3 MPa, falling between the values of the two neat polymers. These enhanced characteristics reveal the two blends' synergistic interaction when combined with a thermo-kinetic mixer. Upon refining the production technique, it becomes possible to achieve compatibility between PP and HDPE, despite their inherent immiscibility as two distinct polymers. This transformation is facilitated through the application of a thermo-kinetic mixer operating at elevated shear rates. This phenomenon has spurred the notion that the substrate for industrial manufacturing could potentially encompass a composite of PP and HDPE, as opposed to exclusively relying on PP.

In this context, ternary nanoblends were conducted by adding GNP into a matrix produced with 75 wt% PP and 25 wt% HDPE to observe the interactions of these polymer blends with GNP. The results of the mechanical properties of ternary nanoblends are shown in Fig. 2. Additionally, Table 1 presents the overall mechanical comparison and improvement of nanoblends compared to PP + HDPE 75/25 and neat PP. When 0.1% GNP was added to the compositions of the blends, a 10% increase in flexural modulus and an 11% increase in tensile modulus were observed compared to PP/HDPE-25. The flexural strength and tensile strength also showed increases of 6 and 5%, respectively. However, it can be observed that as the GNP ratio increases, the improvements in mechanical properties become less significant and reach a plateau at certain points. Table 1 provides a comparison of the mechanical enhancements achieved in relation to pure PP. The utilization of a PP/HDPE blend matrix instead of pure homo PP resulted in significantly greater improvements. This finding holds substantial significance for industrial applications where HDPE offers a relatively cost-effective alternative to PP while simultaneously yielding higher mechanical properties through the synergistic effect of the blend. In industrial applications, where costs and mechanical performance are crucial considerations, the use of HDPE can help as a more economically efficient option

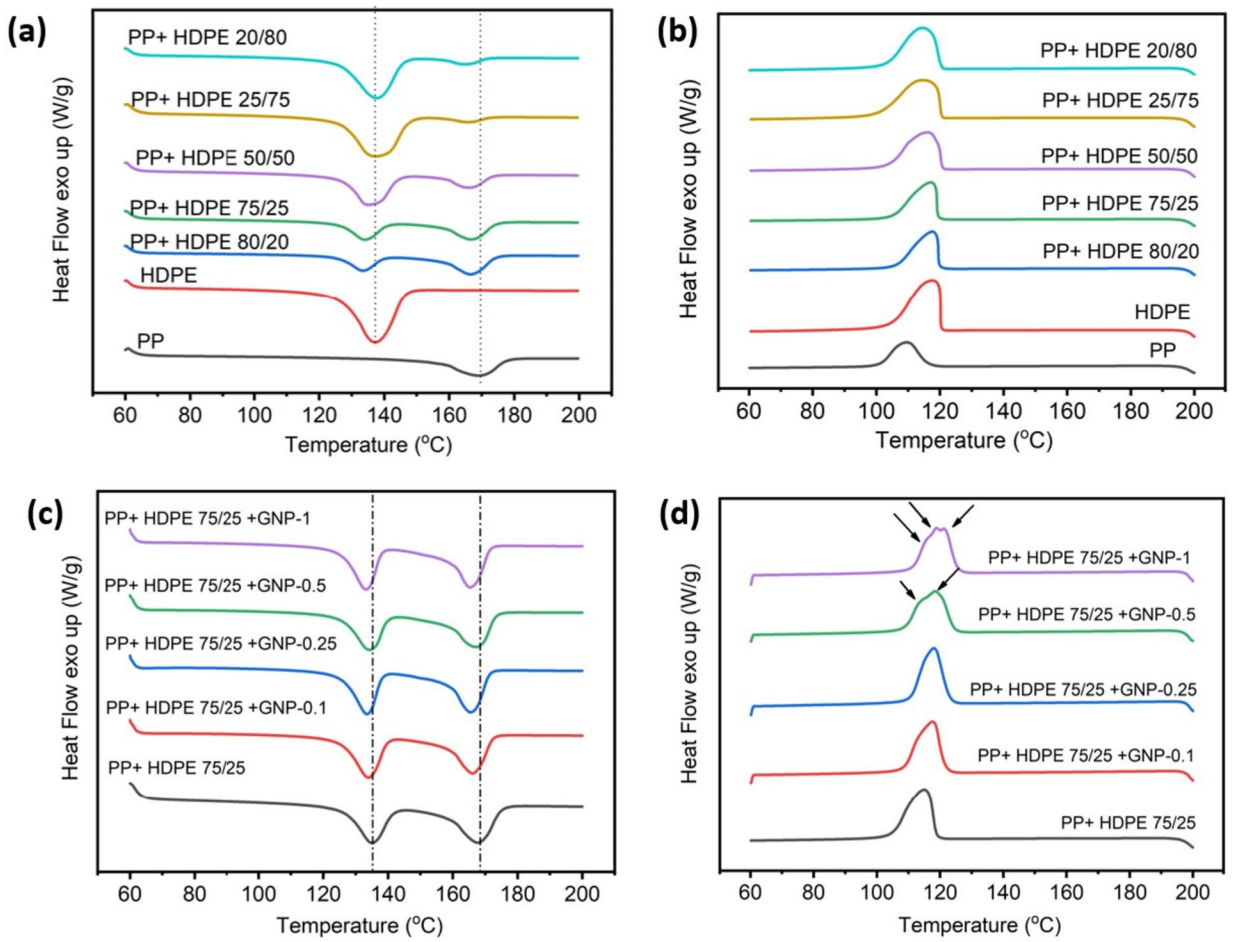

Fig. 4 **a** Second heating, and **b** cooling run of binary blends; **c** second heating, and **d** cooling run of ternary nanoblends

Table 2 Melting and crystallization behavior of binary and ternary nanoblends

	Cooling		2nd Heating				Crystallinity	
	T_c (°C)	ΔH_c (j/g)	T_m of PP (°C)	T_m of HDPE (°C)	ΔH_m of (PP) (j/g)	ΔH_m of (HDPE) (j/g)	Xc of PP (%)	Xc of HDPE (%)
PP	111.2	90.6	169.1	–	90.2	–	43.57	–
PP + HDPE 80/20	117.7	124.9	166.5	133.4	74.7	48.7	36.09	16.9
PP + HDPE 75/25	117.2	131.7	166.7	134.0	70.3	60.1	33.96	20.9
PP + HDPE 50/50	116.1	165.9	166.1	135.1	44.5	114.9	21.50	40.0
PP + HDPE 25/75	114.7	197.7	165.9	137.2	15.6	175.6	7.54	61.18
PP + HDPE 20/80	114.5	181.1	164.9	137.8	19.6	154.6	9.47	53.87
HDPE	117.5	214.3	-	137.0	–	126.9	–	44.22
PP + HDPE 75/25 + GNP-0.1	118.0	124.4	166.0	133.8	53.5	49.2	25.85	17.14
PP + HDPE 75/25 + GNP-0.25	118.3	125.3	165.3	133.4	58.4	45.8	28.21	15.96
PP + HDPE 75/25 + GNP-0.5	118.8	123.0	167.2	134.0	54.3	42.6	26.23	14.84
PP + HDPE 75/25 + GNP-1	119.3	125.3	165.3	133.0	58.s5	45.3	28.26	15.78

compared to homo Polypropylene (PP). Additionally, the combination of HDPE and PP in a blend results in enhanced mechanical properties, and this improvement is emphasized as a synergistic effect, indicating that the combined materials perform better together than individually.

3.2 Viscoelastic Behaviour of Binary Blends and Ternary Nanoblends by DMA

Storage modulus (E′) represents the elastic energy stored by the material and signals the solid-like behavior of materials. In compliance with Fig. 3a, PP has the highest storage modulus compared to HDPE and its HDPE including binary polymer blends. PP storage modulus is superior to HDPE, almost 1.7 times, due to the methyl ($-CH_3$) group in the PP structure, which provides comparatively good mechanical properties by preventing chain rotation [26]. The addition of HDPE at 20 wt% in the PP matrix slightly decreased the storage modulus, and at 25 wt%, it decreased further, which is understandable because PP still predominates as a matrix. The storage modulus of PP + HDPE 50/50 fell in between PP and HDPE due to the equal proportionality. Figure 3d shows the storage modulus of GNP-included ternary polymer nanoblends by taking a reference of PP + HDPE 75/25. The storage modulus of the nanoblends reached the same level with all the GNP addition rates and became independent of the GNP concentration. This shows that with the addition of GNP, the solid-like behavior increased compared to PP + HDPE 75/25. By using 0.1 wt% GNP, similar elastic properties as 1 wt% GNP can be exhibited and there is no need to use higher ratios. Energy dissipation as heat or loss can be examined by loss modulus (E″), and the viscous response of the material can be attained. In line with the Fig. 3a explanation, HDPE showed the highest loss modulus due to easier chain deformation compared to PP, and its addition to PP increased the loss modulus of the binary blends. PP peaks showed its β crystal peaks at around 4–5 °C, and

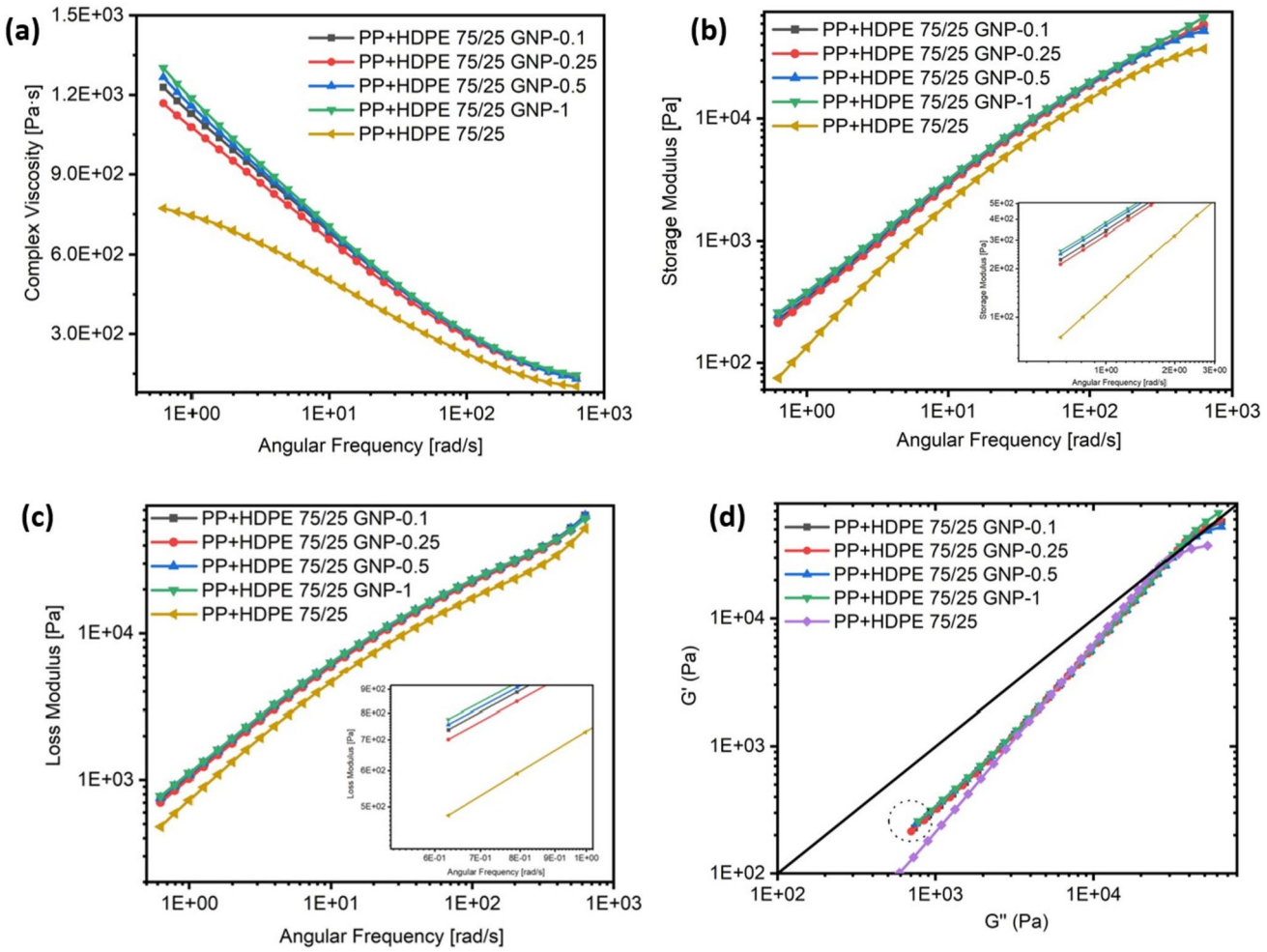

Fig. 5 **a** Complex viscosity, **b** storage modulus, **c** loss modulus, and **d** modified cole–cole pilot of ternary nanoblends

HDPE showed around 39 °C. PP + HDPE 50/50 showed a single peak at around 30 °C, and their liquid-like response concurrently occurred at the same temperature interval. HDPE amount exceeding 50 wt% approached to HDPE due to its predominance in a matrix. In Fig. 3e, loss modulus changes as a function of GNP loading and temperature are given. PP + HDPE 75/25 was compared with its GNP-included ones, and liquid-like behavior underwent a change, unlike their solid-like behavior. 1 wt% GNP included nanoblend decreased the loss modulus at a temperature interval of − 20 °C and 80 °C, which means that stiff GNPs restricted the chain movement in PP + HDPE 75/25 but more dominantly in PP, based on the lowered peak at 4 °C which belongs to PP phase. A slight shift in the maximum peak position of the HDPE phase of PP + HDPE 75/25 + GNP-1 was observed with almost no change in its value. 0.1 wt% GNP included nanoblend has the highest loss modulus peak where it changes when it comes to the HDPE phase. Tan delta values represent the viscous to elastic response (E″/E′) of viscoelastic materials, and the curves after 15 °C in Fig. 3c are also coherent with the storage modulus curves in Fig. 3a. Correspondingly, with the addition of GNP in the blends, tan delta values are also converging mostly in the HDPE phase when comparing Fig. 3c with Fig. 3d. Hereby, it is proper to say that GNP is more dominant in affecting the HDPE phase over PP in the produced nanoblends and/or prefers to locate mostly in the HDPE phase compared to the PP phase.

3.3 Thermal Behaviour of Binary Blends and Ternary Nanoblends by DSC

The thermal behavior of binary and ternary polymer blends was investigated using differential scanning calorimetry (DSC), revealing valuable insights into phase transitions, melting temperatures (Tm), and crystallinity characteristics. The resulting DSC thermograms, as shown in Fig. 4, provided a comprehensive understanding of the blends' thermal properties. Complementary information regarding temperature, enthalpy, and crystallinity for cooling and second heating stages is summarized in Table 2. Examining the binary polymer blends in Fig. 4a, it was observed that HDPE exhibited a Tm of 137 °C, while PP displayed a Tm of 169.1 °C. An increase in the HDPE proportion led to an augmented HDPE melting peak, accompanied by a decrease in the PP peak. Additionally, the incorporation of HDPE caused a reduction of approximately 3 °C in the Tm of PP. Notably, when the HDPE proportion reached 80%, the Tm of PP experienced a further decrease of 4 °C. This downward shift in Tm can be attributed to the occurrence of phase separation between PP and HDPE, influencing the overall melting behavior. In conjunction with the Tm shift, the inclusion of HDPE resulted in a discernible reduction in the crystallinity of PP. Crystallinity calculations, conducted using the heat of fusion values of 287 J/g for 100% crystalline HDPE and 207 J/g for PP [27], showed a decrease in PP crystallinity ranging from 20 to 75% by weight. This decline in crystallinity signifies a corresponding decrease in the relative proportion of crystalline regions, ultimately leading to a shift towards lower temperatures. Analysis of the crystallization

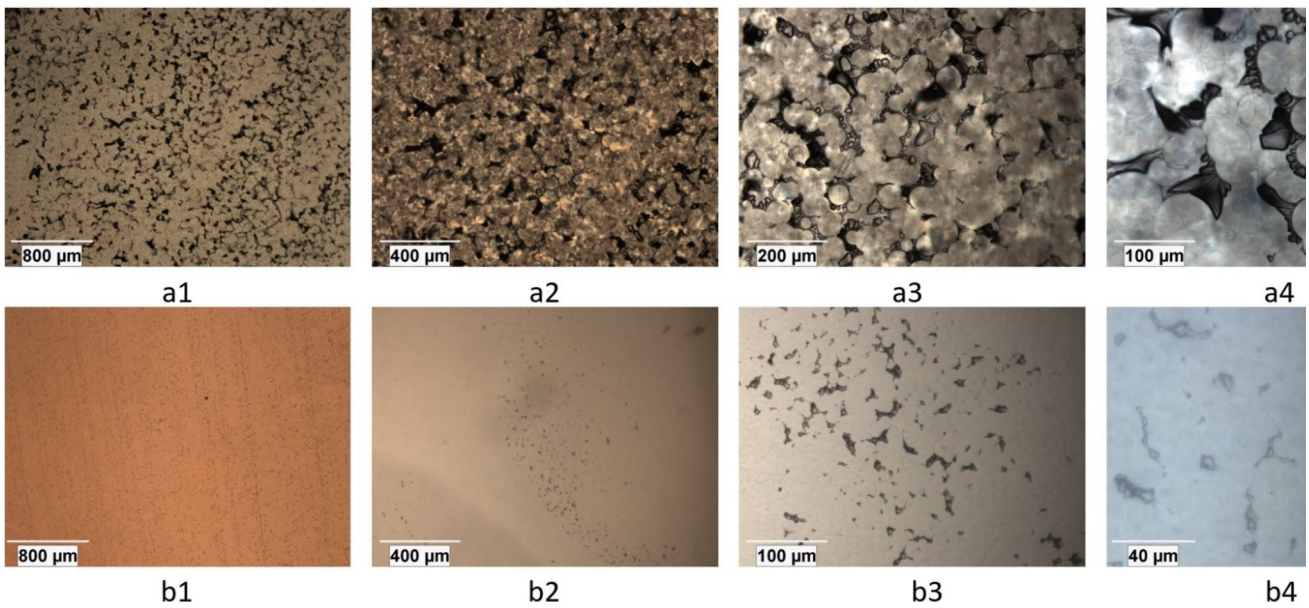

Fig. 6 Semi-polarized optic microscopy images of neat PP (**a1**–**a4**) and neat HDPE (**b1**–**b4**) at different magnifications

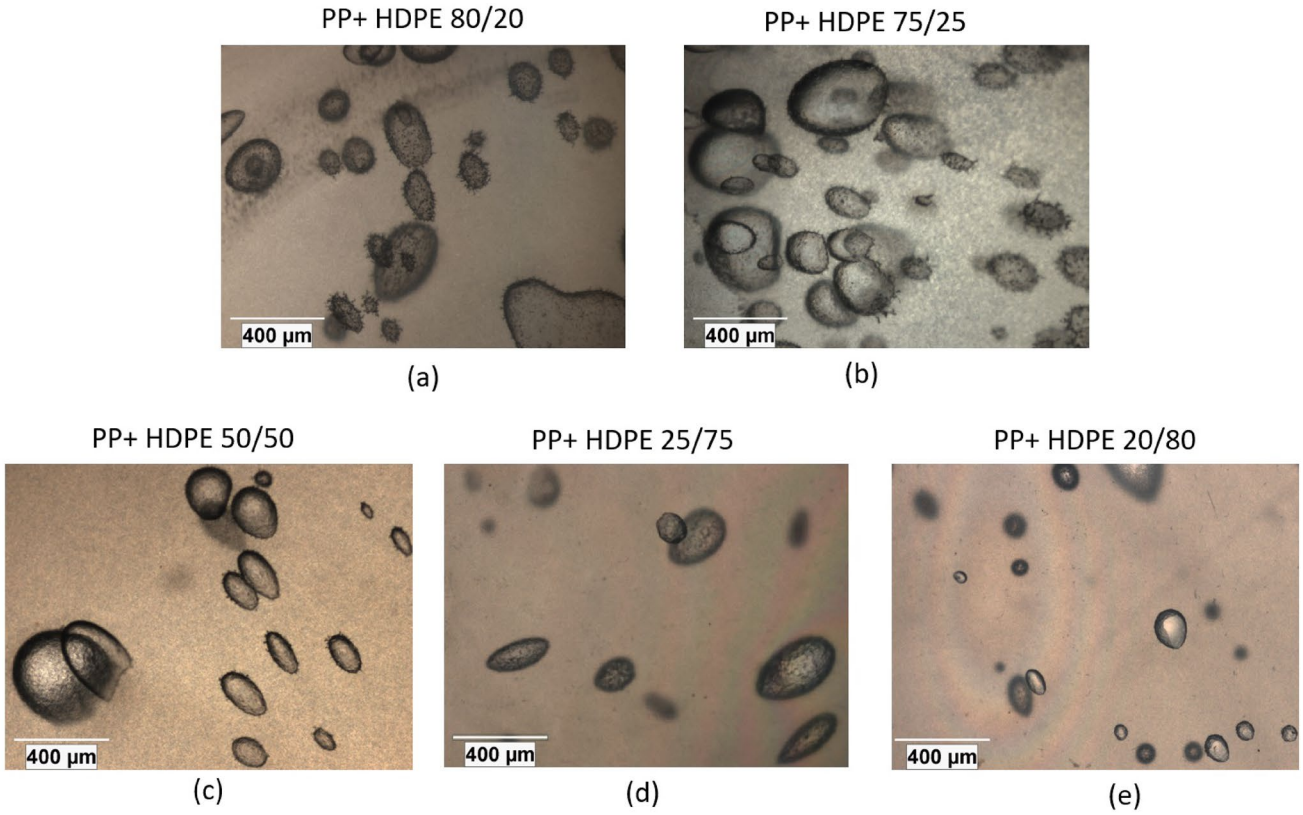

Fig. 7 Semi-polarized optic microscopy images of binary blends

temperatures (Tc) revealed that binary blends exhibited higher Tc values compared to pure PP, indicating alterations in the crystallization behavior induced by the presence of HDPE. Furthermore, in the ternary blends, specifically the PP + HDPE 75/25 compositions, the incorporation of GNP demonstrated an increase in Tc values compared to PP + HDPE 75/25. This observation suggests that GNP may function as a nucleating agent, promoting the formation of smaller and more numerous crystalline structures within the blend. Previous studies have reported the ability of GNP to enhance the Tc of polymers [28]. For the 0.5 wt% GNP and 1 wt% GNP compositions, the crystallization peak started to split, as shown by black arrows in Fig. 4d, indicating more phase separation due to the incorporation of GNP in both PP and HDPE.

3.4 Rheological Investigation of Binary Blends and Ternary Nanoblends by Microscopic Techniques

The rheological investigation of ternary blends is depicted in Fig. 5. A sudden increase in complex viscosity was observed with the addition of a small amount of 0.1 wt% GNP to the PP + HDPE 75/25 blend, as shown in Fig. 5a. This sudden increase indicates good nanoparticle interaction and network formation within the nanoparticles. When the ratio is increased to 0.25 wt% GNP, the viscosity slightly decreases, possibly due to the beginning of GNP agglomeration. Further increases in viscosity were observed with the addition of 0.5 wt% GNP and 1 wt% GNP, indicating a restriction in the matrix's mobility possibly due to the addition of rigid GNPs in higher proportions. The storage modulus and loss modulus values also exhibit a similar pattern of increase. Modified Cole–Cole (Han Plot) can be used to analyze percolation network formation concentration, and a rapid increase in the slope can be attributed to the formation of a nanoparticle network [29]. All GNP concentrations showed a similar deviation from the master curve of PP + HDPE 75/25, demonstrating their ability to improve the rheological behavior of the matrix is similar. The absence of a drastic slope change among the ternary nanoblends might arise from the low content of GNP regarding the studies that showed higher GNP ratios above 2 wt% GNP is needed to reach percolation [1]. Here, below the percolation threshold, it is possible to enrich the mechanical performance of nanocomposites.

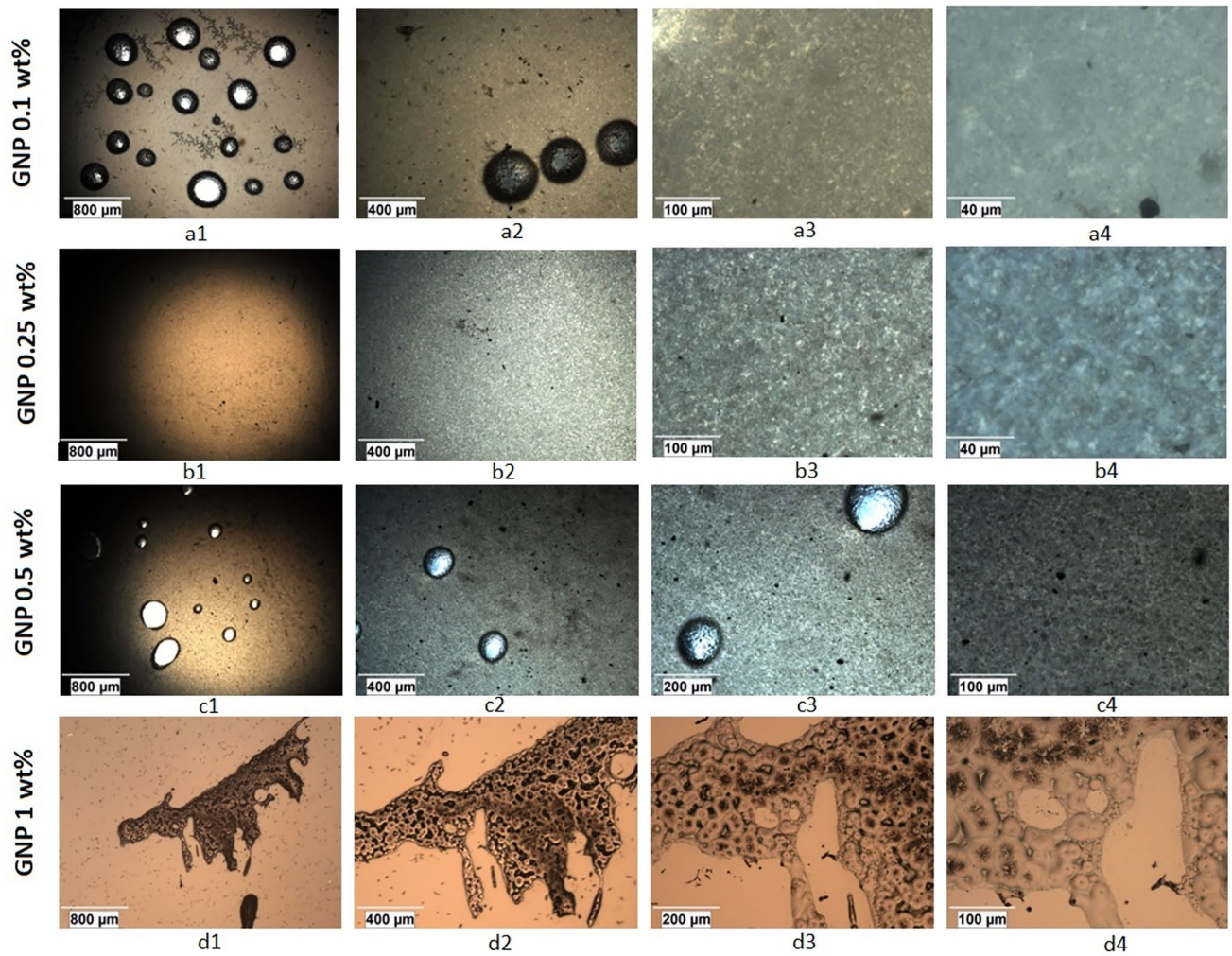

Fig. 8 Semi-polarized optic microscopy images of ternary nanoblends. The polymer blend ratio of PP/HDPE is 75/25 and GNP concentration varies between 0.1–1 wt%

3.5 Morphology Investigation of Binary Blends and Ternary Nanoblends by Microscopic Techniques

Figure 6 presents semi-polarized optical microscope images of neat PP and HDPE. PP formed a high number of spherulites, showed trap nucleation, and formed crystals (a1–a4). PP has a relatively high crystallization rate that leads to the formation of spherulites arising from the growth of crystalline regions. Additionally, isotactic PP, which has a high degree of regularity in the arrangement of polymer chains, tends to form well-defined spherulites [30]. On the other hand, HDPE showed smaller crystallites (b1-b4) compared to PP. HDPE shows slower crystallization compared to PP [31], and therefore its crystal size is smaller.

Optical microscope images of the binary blends are shown in Fig. 7. The large spheres seen in all images in Fig. 7 present PP spheres considering the structures they form in Fig. 6. While PP continues to form its own morphology with non-uniform sphere shapes as in Fig. 7, it starts to form more uniform spheres with the addition of 0.1 wt% GNP, as seen in Fig. 8a1. The circularity of the spheres is remarkably uniform, and there are distinct crystallization patterns observed on the outer regions of these spheres, primarily due to the localized presence of the black GNP. Interestingly, these spheres did not appear at the 0.25 wt% GNP addition. At this GNP loading rate, it might have reached the optimum content for reducing the formation of PP spheres. Upon adding 0.5 wt% GNP, these spheres reappeared but with reduced quantities and diameters compared to 0.1 wt%

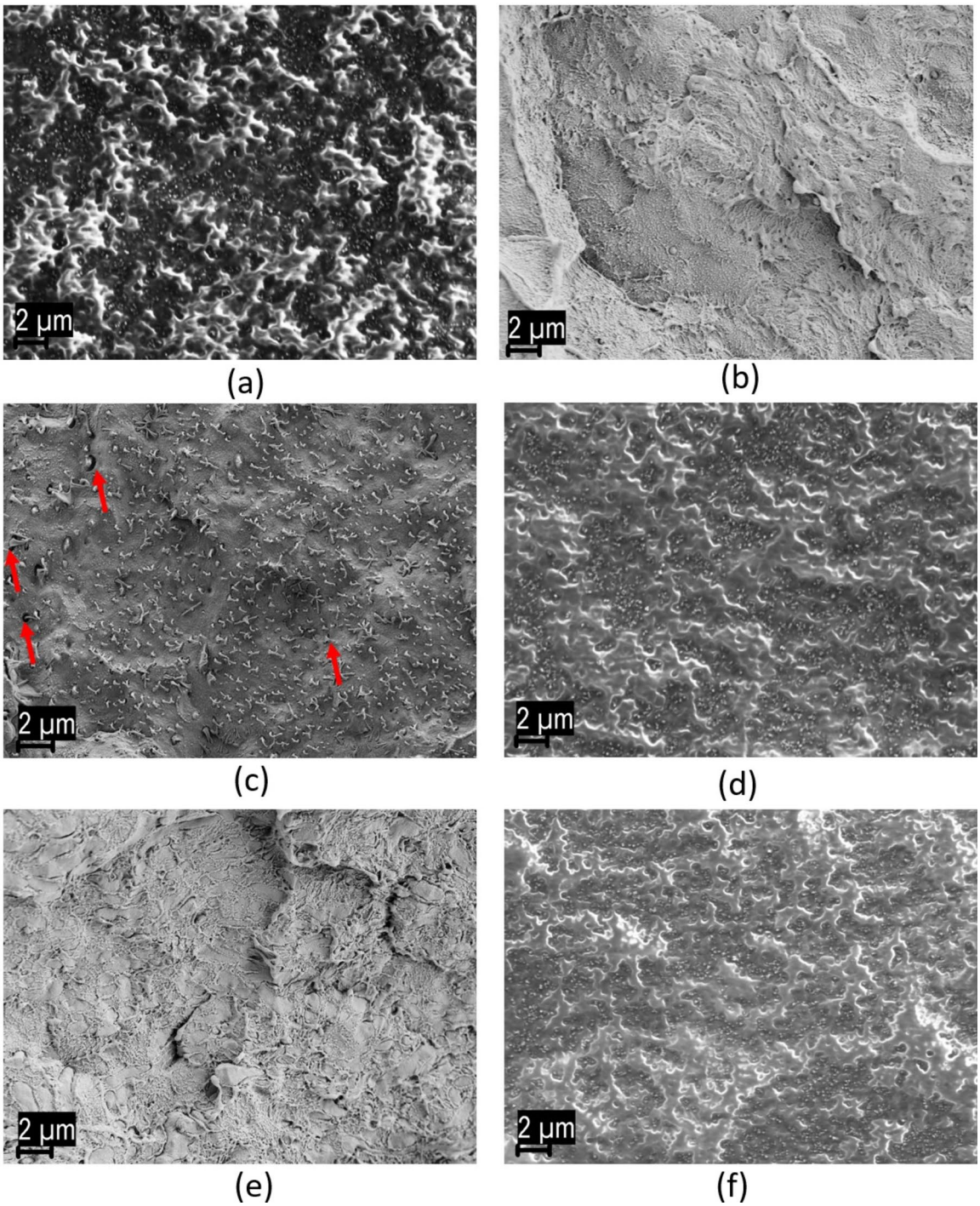

Fig. 9 Cross-sectional analysis of **a** PP, **b** HDPE, **c** PP + HDPE 75/25, **d** PP + HDPE 50/50, **e** PP + HDPE 25/75, and **f** PP + HDPE 75/25 + GNP-0.1 by SEM under 3 kV at 10k magnification

GNP. With the addition of 1 wt% GNP, GNP increased the nucleation rate very quickly, and leopard-patterned morphologies began to form in certain regions as shown in Fig. 8d1–d4. The GNPs initiate the crystallization of polymer phases from various points throughout the matrix. As the GNP content increases, closer magnifications reveal that the matrix droplets also decrease in size.

Figure 9 presents the cross-sectional analyses of neat polymers and their binary and ternary blends to investigate the microstructure. In Fig. 9a, the crystalline structures formed by PP are observed. Figure 9b reveals the presence

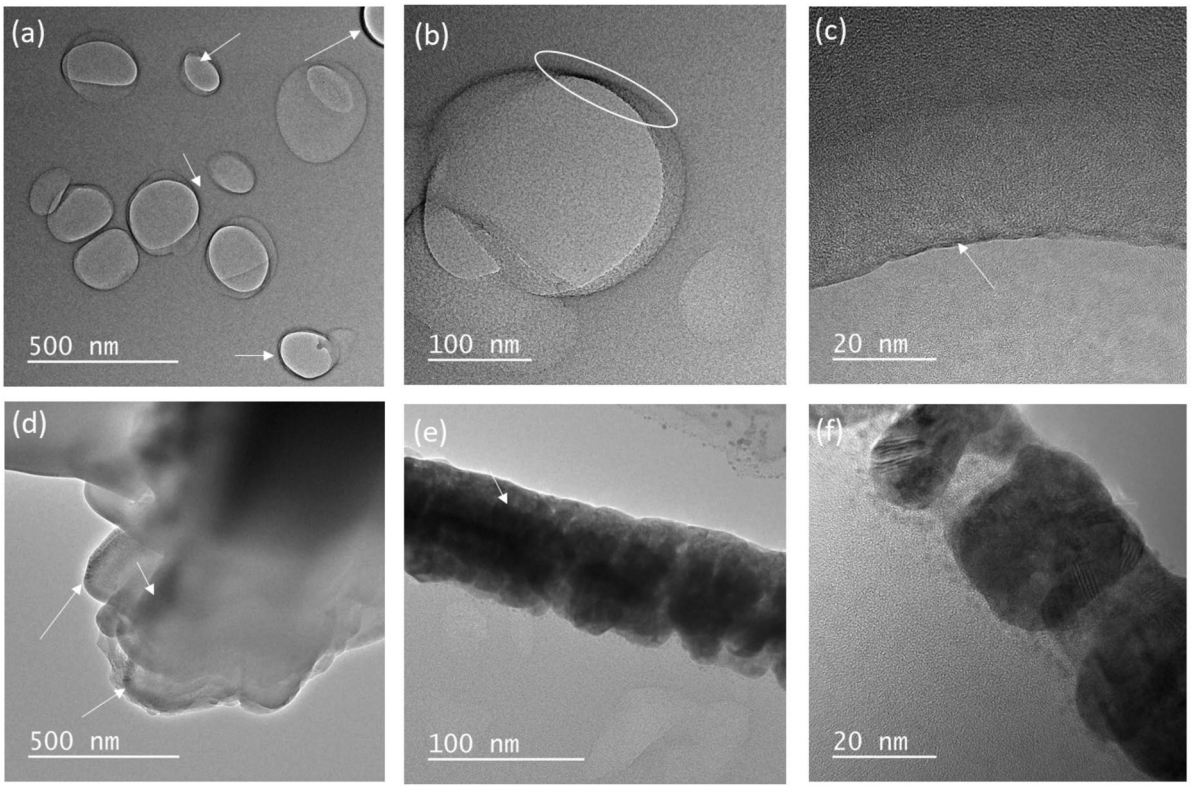

Fig. 10 TEM images of **a–c** PP + HDPE 75/25 + GNP-0.1, **d–f** PP + HDPE 75/25 + GNP-1 ternary nanoblends

of a ductile morphology specific to HDPE. Upon examining the PP + HDPE 75/25 blend (Fig. 9c), it is observed that HDPE protrudes from the matrix in the form of tendrils, possibly indicating interface incompatibility. Notably, are observed in the regions highlighted by red arrows, which are likely a consequence of such interface mismatch. In a 50/50 blend ratio, both PP and HDPE are equally distributed in the matrix, and due to their inherent incompatibility, PP initiates crystallization within its domains, thus exhibiting its distinct phases. With an increased HDPE content of 75%, HDPE becomes the major phase, manifesting its dominance and leading to a fracture behavior reminiscent of neat HDPE, displaying a more flexible nature. Figure 9f showcases the sample of PP + HDPE 75/25 + GNP-0.1, where 0.1 wt% GNP is added. Notably, compared to Fig. 9c, the void structures are no longer observed, and the crystalline structure of the PP phase reappears. This observation suggests that GNP contributes to localized PP crystallization at the blend interface and within the PP matrix, indicating its potential role in enhancing crystalline characteristics.

The TEM micrographs of PP + HDPE 75/25 + GNP-0.1 and PP + HDPE 75/25 + GNP-1 ternary nanoblends are depicted in Fig. 10. The presence of dispersed HDPE droplets surrounded by the PP matrix can be seen in Fig. 10a. The GNP, represented by black dots indicated by arrows, is observed precisely at the interface between the PP and HDPE phases in Fig. 10a and closer view in Fig. 10b and c. Conversely, when examining the blend with a 1 wt% GNP content, a higher concentration of GNP particles infiltrating the interphases becomes evident. A closer view in Fig. 10e reveals significant agglomeration forming clusters with a size of approximately 75 nm and resulting in a visually darker image due to GNP overlap. Consequently, successful localization of 0.1 wt% GNP at the PP + HDPE 75/25 interface was observed, while higher GNP ratios led to undesirable agglomeration.

4 Conclusion and Future Outlook

The current study achieved to provide a cost-effective blend formulation by utilizing a PP/HDPE matrix and improving its mechanical behavior through the incorporation of GNP via an adaptable processing technique. By utilizing a high shear rate thermo-kinetic mixer and incorporating upcycled graphene nanoplatelets (GNP) through interface engineering, the researchers successfully addressed the entropy barrier between PP and HDPE. The results demonstrated that careful selection of polymer weight fraction and optimized GNP loading facilitated the localization of GNP at the blend

interface, leading to notable improvements in mechanical performance. The addition of 0.1 wt% GNP resulted in a significant 38% increase in tensile modulus, along with 39 and 22% increases in flexural modulus and flexural strength, respectively. Rheological analysis indicated that the inclusion of GNP in the nanoblends enhanced the complex viscosity, storage modulus, and loss modulus, indicating the formation of a nanoparticle network at low GNP contents. Morphological studies confirmed the successful localization of GNP at the blend interface, leading to improved crystallization patterns and reduced void structures.

The successful incorporation of upcycled graphene nanoplatelets (GNP) in PP/HDPE blend systems through a high shear rate thermo-kinetic mixer opens promising avenues for future research and applications. Investigating the influence of different processing parameters, mixing techniques, and GNP modifications on the blend morphology and properties can provide valuable insights for tailoring materials with specific characteristics. The industrial scalability of the developed blend formulation and processing technique assesses their feasibility for large-scale production. This could involve evaluating the economic viability, processing efficiency, and scalability of the thermo-kinetic mixer in comparison to conventional extrusion methods. Additionally, the introduction of waste tire-driven GNP into thermoplastic blends not only enhances their recyclability but also significantly elevates their mechanical properties. This approach offers a practical solution for both waste reduction and the development of high-performance, eco-friendly materials.

As we explore the potential of GNP-integrated polymer blends, the idea of incorporating GNP into recycled polymer blends emerges as a promising prospect. This concept aligns with the broader theme of sustainable material development, wherein recycled polymer blends, enriched with GNP, could present a dual advantage—improved mechanical properties and a second life for recycled materials.

Acknowledgements The authors would like to thank Arçelik A.S for supporting the current industrial project and supplying polymer materials. The project is also supported by the Scientific and Technological Research Council of Turkey (TUBITAK) with project number 118C046 and 5200117 project code. The authors would like to thank Sabancı University Nanotechnology Research and Application Center – SUNUM for providing TEM analysis.

Author Contributions GŞD: Investigation, Conceptualization, Methodology, Writing—original draft. BSO: Supervision, Funding Acquisition, Conceptualization, Writing—review & editing.

Funding Open access funding provided by the Scientific and Technological Research Council of Türkiye (TÜBİTAK). The author(s) received no financial support for the research, authorship, and/or publication of this article.

Data Availability No datasets were generated or analysed during the current study.

Declarations

Conflict of interest The author(s) declared no potential conflicts of interest concerning the research, authorship, and/or publication of this article.

Open Access This article is licensed under a Creative Commons Attribution 4.0 International License, which permits use, sharing, adaptation, distribution and reproduction in any medium or format, as long as you give appropriate credit to the original author(s) and the source, provide a link to the Creative Commons licence, and indicate if changes were made. The images or other third party material in this article are included in the article's Creative Commons licence, unless indicated otherwise in a credit line to the material. If material is not included in the article's Creative Commons licence and your intended use is not permitted by statutory regulation or exceeds the permitted use, you will need to obtain permission directly from the copyright holder. To view a copy of this licence, visit http://creativecommons.org/licenses/by/4.0/.

References

1. A. Kol, S. Kenig, N. Naveh, Silane-modified graphene oxide as a compatibilizer and reinforcing nanoparticle for Immiscible PP/PA blends. Polym. Eng. Sci. (2020). https://doi.org/10.1002/pen.25271
2. N.Z. Tomić, A.D. Marinković, in *Compatibilization of polymer blends by the addition of graft copolymers*, Compatibilization of Polymer Blends (Elsevier, 2020) pp. 103–144
3. M.S. De Luna, G. Filippone, Effects of nanoparticles on the morphology of immiscible polymer blends-challenges and opportunities. Eur. Polym. J. (2016). https://doi.org/10.1016/j.eurpolymj.2016.02.023
4. A. Graziano, C. Garcia, S. Jaffer, J. Tjong, M. Sain, Novel functional graphene and its thermodynamic interfacial localization in biphasic polyolefin systems for advanced lightweight applications. Compos. Sci. Technol. (2020). https://doi.org/10.1016/j.compscitech.2019.107958
5. A. Graziano, O.A.T. Dias, C. Garcia, S. Jaffer, J. Tjong, M. Sain, Impact of reduced graphene oxide on structure and properties of polyethylene rich binary systems for performance-based applications. Polym. (Guildf) **202**, 122622 (2020). https://doi.org/10.1016/j.polymer.2020.122622
6. A. Graziano, C. Garcia, J. Tjong, W. Yang, M. Sain, Functionally tuned nanolayered graphene as reinforcement of polyethylene nanocomposites for lightweight transportation industry. Carbon N Y. **169**, 99–110 (2020). https://doi.org/10.1016/j.carbon.2020.07.040
7. A.R. Ajitha, L.P. Mathew, S. Thomas, in *Compatibilization of polymer blends by micro and nanofillers*, Compatibilization of Polymer Blends (Elsevier, 2020). pp. 179–203. https://doi.org/10.1016/B978-0-12-816006-0.00006-2
8. L. Bai, R. Sharma, X. Cheng, C.W. Macosko, Kinetic control of graphene localization in co-continuous polymer blends via melt compounding. Langmuir **34**(3), 1073–1083 (2018).
9. F. Abbasi, D.A. Shojaei, S.M. Bellah, The compatibilization effect of exfoliated graphene on rheology, morphology, and mechanical and thermal properties of immiscible polypropylene/polystyrene (PP/PS) polymer blends. J. Thermoplast. Compos. Mater. (2019). https://doi.org/10.1177/0892705718797153

10. P. Feng, J. Jia, S. Peng, W. Yang, S. Bin, C. Shuai, Graphene oxide-driven interfacial coupling in laser 3D printed PEEK/PVA scaffolds for bone regeneration. Virtual Phys. Prototype. **15**(2), 211–226 (2020). https://doi.org/10.1080/17452759.2020.1719457
11. M. Liebscher, M.O. Blais, P. Pötschke, G. Heinrich, A morphological study on the dispersion and selective localization behavior of graphene nanoplatelets in immiscible polymer blends of PC and SAN. Polymer (2013). https://doi.org/10.1016/j.polymer.2013.08.009
12. R. Doufnoune, T. Baouz, S. Bouchareb, Influence of functionalized reduced graphene oxide and compatibilizer on mechanical, thermal and morphological properties of polypropylene/polybutene-1 (PP/PB-1) blends. J. Adhes. Sci. Technol. ISSN. **33**(16), 1729–1757 (2019). https://doi.org/10.1080/01694243.2019.1611367
13. Y. Shen, T.T. Zhang, J.H. Yang, N. Zhang, T. Huang, Y. Wang, Selective localization of reduced graphene oxides at the interface of PLA/EVA blend and its resultant electrical resistivity. Polym. Compos. **38**(9), 1982–1991 (2017). https://doi.org/10.1002/pc.23769
14. M. Bera, U. Saha, A. Bhardwaj, P.K. Maji, Reduced graphene oxide (RGO) -induced compatibilization and reinforcement of poly (vinylidene fluoride) (PVDF)–thermoplastic polyurethane (TPU) binary polymer blend. J. Appl. Polym. Sci. **47010**, 1–13 (2019). https://doi.org/10.1002/app.47010
15. C. Tu, K. Nagata, Dependence of electrical conductivity on phase morphology for graphene selectively located at the interface of polypropylene/polyethylene composites. Nanomaterials (2022). https://doi.org/10.3390/nano12030509
16. Y. Ding, C. Abeykoon, Y.S. Perera, The effects of extrusion parameters and blend composition on the mechanical, rheological and thermal properties of LDPE/PS/PMMA ternary polymer blends,. Adv. Ind. Manuf. Eng, (2021). https://doi.org/10.1016/j.aime.2021.100067
17. D.N. Trivedi, N.V. Rachchh, Graphene and its application in thermoplastic polymers as nano-filler- a review. Polymer (Guildf) (2021). https://doi.org/10.1016/j.polymer.2021.124486
18. B. Cetiner, G.S. Dundar, Y. Yusufoglu, B.S. Okan, Sustainable engineered design and scalable manufacturing of upcycled graphene reinforced polylactic acid/polyurethane blend composites having shape memory behavior. Polym. (Basel) (2023). https://doi.org/10.3390/polym15051085
19. H. Kamalvand, P. Rajaee, An experimental investigation of the tensile, fracture and microstructural characteristics of ABS/SBS reinforced with HNTs. Polym. Compos. (2023). https://doi.org/10.1002/pc.27573
20. G. Şahin Dündar, B. Saner Okan, An efficient interface model to develop scalable methodology of melt processing of polypropylene with graphene oxide produced by an improved and eco-friendly electrochemical exfoliation. J. Appl. Polym. Sci. **140**(2), 1–14 (2023). https://doi.org/10.1002/app.53282
21. V. Pandey, H. Chen, M. Maia, J. Ma, Extension-dominated improved dispersive mixing in single-screw extrusion. Part 2 : Comparative analysis with twin-screw extruder. J. Appl. Polym. Sci. (2020). https://doi.org/10.1002/app.49765
22. E. Sasimowski, Ł. Majewski, M. Grochowicz, Efficiency of twin-screw extrusion of biodegradable poly (butylene succinate)-wheat bran blend. Materials **14**(2), 424 (2021).
23. L. Techawinyutham, J. Tengsuthiwat, R. Srisuk, Recycled LDPE / PETG blends and HDPE / PETG blends: mechanical, thermal, and rheological properties. J. Mater. Res. Technol. **15**, 2445–2458 (2021). https://doi.org/10.1016/j.jmrt.2021.09.052
24. M. Ahmadlouydarab, M. Chamkouri, H. Chamkouri, Compatibilization of immiscible polymer blends (R – PET / PP) by adding PP–g–MA as compatibilizer: analysis of phase morphology and mechanical properties. Polym. Bull. (2020). https://doi.org/10.1007/s00289-019-03054-w
25. J. Chen et al., Control of graphene nanoplatelets at the interface of the co-continuous polypropylene/polyamides 6 blend under the elongational flow. Eur. Polym. J. (2022). https://doi.org/10.1016/j.eurpolymj.2022.111703
26. A.H. Awad, R. El Gamasy, A. Abd, E. Wahab, M.H. Abdellatif, Mechanical and physical properties of PP and HDPE. Eng. Sci. (2019). https://doi.org/10.11648/j.es.20190402.12
27. S. Jose et al., Phase morphology, crystallization behaviour and mechanical properties of isotactic polypropylene/high density polyethylene blends. Eur. Polym. J. **40**(9), 2105–2115 (2004). https://doi.org/10.1016/j.eurpolymj.2004.02.026
28. J. Bian, Z. Jun, H. Lan, X. Zhou, W. Qiang, X. Wei, Composites: part a thermal and mechanical properties of polypropylene nanocomposites reinforced with nano-SiO_2 functionalized graphene oxide. Compos. Part. A **97**, 120–127 (2017). https://doi.org/10.1016/j.compositesa.2017.01.002
29. E. Vatansever, D. Arslan, D.S. Sarul, Y. Kahraman, M. Nofar, Effects of molecular weight and crystallizability of polylactide on the cellulose nanocrystal dispersion quality in their nanocomposites. Int. J. Biol. Macromol. **154**, 276–290 (2020). https://doi.org/10.1016/j.ijbiomac.2020.03.115
30. C. Hu, C. Li, L. Feng, X. Gu, J. Duan, C. Zhang, Modification of the crystallization behavior of Isotactic polypropylene by grafting styrene segments. Ind. Eng. Chem. Res. (2022). https://doi.org/10.1021/acs.iecr.2c00738
31. K.M. Seven, J.M. Cogen, J.F. Gilchrist, Nucleating agents for high-density polyethylene—a review. Polym. Eng. Sci. (2016). https://doi.org/10.1002/pen

Publisher's Note Springer Nature remains neutral with regard to jurisdictional claims in published maps and institutional affiliations.